



Universiteit
Leiden
The Netherlands

Advances in the imaging of pituitary tumors

MacFarlane, J.; Bashari, W.A.; Senanayake, R.; Gillett, D.; Meulen, M. van der; Powlson, A.S.; ... ; Gurnell, M.

Citation

MacFarlane, J., Bashari, W. A., Senanayake, R., Gillett, D., Meulen, M. van der, Powlson, A. S., ... Gurnell, M. (2020). Advances in the imaging of pituitary tumors. *Endocrinology And Metabolism Clinics Of North America*, 49(3), 357-373. doi:10.1016/j.ecl.2020.06.002

Version: Publisher's Version

License: [Creative Commons CC BY 4.0 license](https://creativecommons.org/licenses/by/4.0/)

Downloaded from: <https://hdl.handle.net/1887/3627408>

Note: To cite this publication please use the final published version (if applicable).

Advances in the Imaging of Pituitary Tumors



James MacFarlane, MRCPUK^{a,1}, Waiel A. Bashari, MSc, MRCPUK^{a,1},
Russell Senanayake, MSc, MRCPUK^{a,1}, Daniel Gillett, MSc^{a,b},
Merel van der Meulen, BSc^a, Andrew S. Powlson, MRCPUK^a,
Angelos Koliass, PhD, FRCS^c, Olympia Koulouri, PhD, MRCPUK^a,
Mark Gurnell, PhD, FRCP^{a,*}

KEYWORDS

• Pituitary adenoma • MRI • PET/CT • ¹¹C-methionine • Met-PET/MR^{CR}

KEY POINTS

- MRI remains the primary modality for imaging pituitary tumors (pituitary adenomas [PA]).
- Conventional magnetic resonance (MR) sequences provide sufficient information to guide management in most patients, but can lack sensitivity and specificity for (i) detection of microadenomas; or (ii) identification of the site or sites of residual/recurrent disease following primary therapy.
- Alternative MR sequences may aid characterization of specific tumor traits (eg, tumoral consistency; presence of apoplexy; invasion of surrounding structures).
- Several different radiotracers have been investigated for molecular imaging of pituitary tumors with varying success.
- ¹¹C-methionine PET coregistered with volumetric (1-mm slice) MRI (Met-PET/MR^{CR}) can aid accurate localization of microadenomas/picoadenomas of all PA subtypes, identify sites of recurrent or incompletely resected disease, and distinguish from postoperative change (eg, acromegaly, Cushing disease), and augment radiotherapy planning in selected cases.

Funding sources: J. MacFarlane, W.A. Bashari, R. Senanayake, D. Gillett, A. Koliass, O. Koulouri, and M. Gurnell are supported by the Cambridge NIHR Biomedical Research Centre; this work was also supported by a project grant from the Evelyn Trust (W.A. Bashari, O. Koulouri, M. Gurnell).

^a Cambridge Endocrine Molecular Imaging Group, Metabolic Research Laboratories, Wellcome Trust-MRC Institute of Metabolic Science, University of Cambridge, National Institute for Health Research, Cambridge Biomedical Research Centre, Addenbrooke's Hospital, Hills Road, Cambridge CB2 0QQ, UK; ^b Department of Nuclear Medicine, Addenbrooke's Hospital, Hills Road, Cambridge CB2 0QQ, UK; ^c Division of Neurosurgery, Department of Clinical Neurosciences, University of Cambridge & Addenbrooke's Hospital, Cambridge CB2 0QQ, UK

¹ These authors contributed equally to this work.

* Corresponding author.

E-mail address: mg299@medschl.cam.ac.uk

Endocrinol Metab Clin N Am 49 (2020) 357–373

<https://doi.org/10.1016/j.ec.2020.06.002>

0889-8529/20/© 2020 Elsevier Inc. All rights reserved.

endo.theclinics.com

INTRODUCTION

Pituitary adenomas (PA) are typically benign, slow-growing tumors of the adenohypophysis, which come to attention because of associated endocrine dysfunction (eg, hyperprolactinemia, hypercortisolism, acromegaly/gigantism, hypopituitarism) or mass effect (eg, compression of the optic chiasm or cranial nerves in the wall of the cavernous sinus), or when they are discovered incidentally during cross-sectional imaging of the brain performed for a separate indication.¹

Pituitary incidentalomas are a relatively common finding in the general population, with a large metaanalysis of autopsy series suggesting a mean prevalence of 10.7% (range 1.5%–31%).² These findings are broadly consistent with MRI studies of the sella and parasellar regions, which identify abnormalities in as many as 10% to 38% of subjects in unselected cohorts.^{3,4} Most of these are microadenomas, and most do not result in endocrine dysfunction.⁵ In contrast, clinically relevant PA have been estimated to affect between 1:1064 and 1:1200 of the general population.^{6,7}

Modern management of PA is ideally overseen by a specialist multidisciplinary team comprising neuroendocrinology, neurosurgery, otolaryngology, neuroradiology, neuropathology, neuroophthalmology and neurooncology.⁸ Cross-sectional imaging (MRI and/or computed tomography [CT]) of the sella and parasellar regions is central to effective decision making and may be the major determinant of whether a patient is offered surgery, radiotherapy, medical therapy, or surveillance. For most cases, MRI remains the primary imaging modality and distinguishes the adenoma from normal pituitary tissue and adjacent structures.^{9,10} However, in a small but important subgroup of patients, conventional pituitary imaging is not informative. For example, although incidentalomas are a common finding in the general population, paradoxically some functioning microadenomas (including 30%–40% of corticotroph adenomas) are not readily visualized on standard pituitary magnetic resonance (MR) sequences.¹¹ Similarly, following transsphenoidal surgery (TSS), sites of residual or recurrent disease may not be evident or readily distinguished from posttreatment changes.¹² In these contexts, the decision then lies between “blind” surgical (re-)exploration, long-term (in some cases life-long) medical therapy, radiotherapy, or even a combination of approaches, each with their own limitations with respect to the likelihood and time to achieving disease control, risk of inducing hypopituitarism, and causation of other adverse effects.

Accordingly, several novel approaches to pituitary imaging have been proposed, largely based on the deployment of alternative MR sequences or novel techniques for image analysis, with the aims of (i) improving diagnostic resolution, (ii) informing pretreatment planning, and (iii) predicting likely responses to different therapeutic strategies. In addition, a role for molecular imaging, with its ability to confirm/localize sites of functioning active tumor, is gaining prominence and may be particularly valuable when cross-sectional imaging remains equivocal. Here, the authors consider how these advances might be integrated into modern imaging algorithms to better inform the management of patients with PA.

MRI

In a patient in whom a PA is suspected, dedicated MRI of the sella and parasellar regions should be performed to confirm the site and size of the tumor and its relationship to surrounding important structures. CT may offer important supplementary information in some cases (eg, defining the extent of bony erosion with larger tumors; confirming/excluding the presence of calcification), and modern thin-slice CT is a reasonable alternative for those unable or unwilling to undergo MRI.¹⁰

Standard Clinical Pituitary MRI

Spin-echo (SE) pulse sequences are one of the earliest developed and still widely used of all MRI pulse sequences and remain a cornerstone of modern pituitary imaging. Although practice varies from center to center, routine clinical pituitary MRI protocols (using a 1.5 Tesla [1.5 T] or 3 T scanner) typically include the following:

- Precontrast T1-weighted SE and T2-weighted fast SE (FSE) coronal and sagittal sections with thin slices (typically 2–3 mm)
- Postcontrast T1-weighted SE coronal and sagittal sections with thin slices

The addition of axial images may also be helpful in some cases and allows for more complete evaluation of the posterior pituitary gland.¹³

The normal anterior pituitary gland is isointense to gray matter on noncontrast T1- and T2-weighted SE/FSE sequences; the posterior lobe demonstrates high T1 signal, but is hypointense on T2. Following injection of contrast, the infundibulum and gland progressively enhance (homogeneously). Contrast uptake by PA is typically slower, resulting in delayed enhancement and washout.^{10,14}

For cases without a clear abnormality on MRI, but in whom a lesion is strongly suspected on clinical grounds (eg, ACTH-dependent Cushing syndrome with biochemical and/or petrosal sinus catheter evidence of a central origin), dynamic contrast-enhanced MRI (using T1-weighted sequences precontrast and immediately postcontrast administration) may help identify the site of a microadenoma. However, gradient echo (for example, spoiled gradient echo, [fast] spoiled gradient recalled [FSPGR/SPGR]), which allows imaging with a 1-mm-slice interval, has been suggested to offer greater sensitivity for localizing microadenomas in the context of Cushing disease.^{15,16}

The most commonly used contrast agent for pituitary imaging is gadolinium, a naturally occurring lanthanide with strong paramagnetic properties (owing to 7 unpaired electrons). In its free form, gadolinium is toxic and must therefore be chelated to a carrier ligand to permit safe clinical use. Recently, however, concern has arisen regarding the potential for gadolinium deposition in the central nervous system even in patients with normal renal function,^{17,18} which presents a particular challenge for pituitary endocrinologists and their patients given the often long-term requirement for periodic surveillance imaging.¹⁹ It is therefore important that the need for contrast enhancement is carefully considered whenever imaging of the sella and parasellar regions is requested. For example, in a patient with a well-defined intrasellar tumor remnant following primary surgery for a nonfunctioning PA, and which is well visualized on non-contrast MRI, the inclusion of postgadolinium sequences is likely to add little to the clinical decision-making process; if there are concerns regarding tumor enlargement on noncontrast T1- and T2-weighted images, the patient can be recalled for further assessment.

Similarly, attention has recently been drawn to those clinical settings in which T2-weighted MRI can afford comparable or even superior information to that provided by T1-weighted postcontrast imaging,²⁰ thus potentially avoiding the need for initial and/or repeat gadolinium administration (**Fig. 1, Table 1**).

Alternative Pituitary Magnetic Resonance Sequences/Techniques

An increasing array of MR sequences has been adapted for use in pituitary disease. In addition, as the availability of higher-field-strength MRI systems (eg, 7 T) increases, potential applications in patients with PA are being increasingly explored. Currently, most of these approaches remain outside standard clinical protocols for imaging of

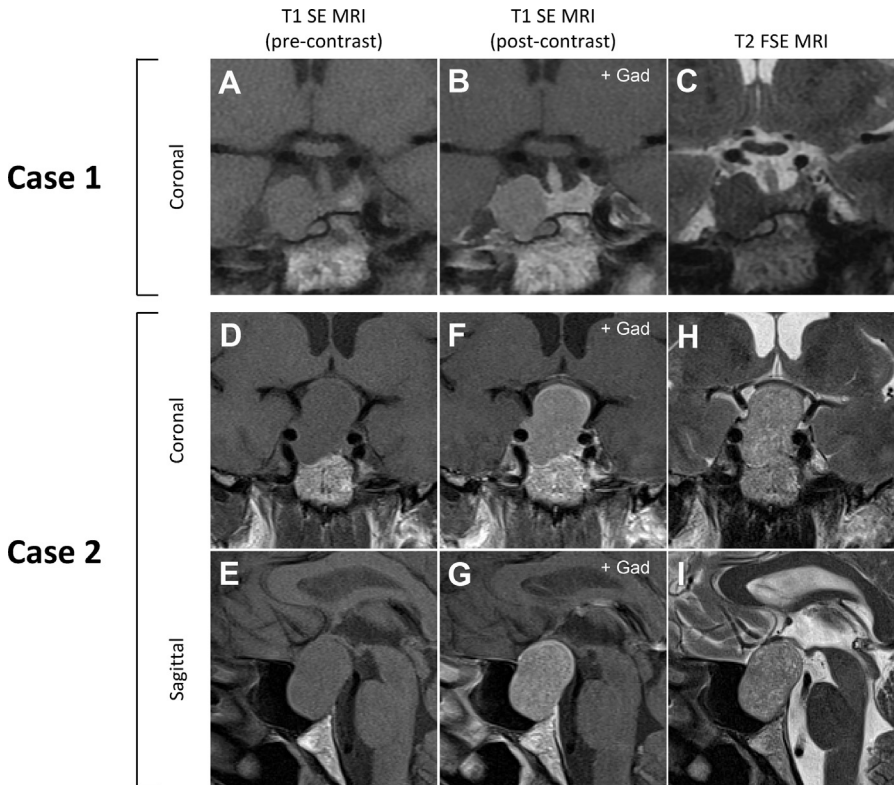


Fig. 1. Prediction of pituitary tumor phenotype based on T2-weighted MRI appearances. (A–C) T1 SE (precontrast and postcontrast) and T2 FSE MRI in a patient with acromegaly, demonstrating a right-sided macroadenoma; the tumor is hypointense on T2 sequences when compared with the adjacent temporal lobe, which has been linked with somatostatin analogue responsiveness and a densely granulated appearance on histology. (D–I) T1 SE (precontrast and postcontrast) and T2-weighted FSE MRI showing a macroadenoma with suprasellar extension in a patient who presented with visual loss, but no clinical or biochemical features of hypercortisolism; the tumor exhibits multiple microcysts (focal small areas of high intensity) on the T2 images. Gad, gadolinium; T1, T1 weighted; T2, T2 weighted.

the sella and parasellar regions, but may be requested when conventional sequences leave important questions unanswered. These sequences can be broadly considered under the following 3 indications (**Table 2**):

- A. To aid a diagnosis
- B. To help inform preoperative assessment
- C. To predict likely treatment outcomes

Advances in Image Analysis

Novel approaches to image analysis are also being translated from other disease areas, allowing additional information to be derived from existing pituitary MR protocols. For example, in a study of 89 patients who had undergone TSS, and for whom the tumor Ki-67 proliferation index was available, machine learning analysis of texture-derived parameters from preoperative T2-weighted MRI allowed prediction of which tumors would

Table 1 Utility of T2-weighted magnetic resonance sequences in pituitary imaging		
T2-weighted MRI Appearance	Differential Diagnosis	References
Hypointense	Rathke cleft cyst Hypointensity observed in one-third of cases, although hypointense intracystic nodules are present in up to 70% of cases, which are virtually pathognomonic	20
	GH-secreting PA (>50%) Hypointensity typically associated with: <ul style="list-style-type: none"> • Smaller tumors • Lower tendency to CSI • Greater SSA responsiveness Prolactinoma Hypointensity seen in a subset of cases (up to 20%, especially in men); unclear whether this predicts resistance to DA therapy; may indicate greater likelihood of growth during pregnancy	20,59,60 61
Hyperintense (often strongly)	Hypophysitis For example, lymphocytic/autoimmune, immunotherapy-related or IgG4 disease	20
Hyperintense	Rathke cleft cyst Hyperintensity observed in 70% of cases	20
Hyperintense (mild-moderate)	Prolactinoma (especially microadenomas) In general, degree of hyperintensity does not reliably predict response to DA therapy; accentuation of hyperintensity may occur following DA therapy	61
Hyperintense/isointense	GH-secreting PA Hyperintensity/isointensity associated with: <ul style="list-style-type: none"> • Larger tumors • Greater tendency to CSI • Less SSA responsiveness 	20,59,60
Microcystic pattern	Silent corticotroph (macro)adenoma Multiple microcysts (small areas of high-intensity signal covering at least 25% of the tumor) observed in 50%–75% of cases	20,62

Abbreviations: CSI, cavernous sinus invasion; GH, growth hormone; IgG4, immunoglobulin subtype 4. Data from Refs.^{20,59–62}

exhibit a high Ki-67 labeling index.²¹ The adoption of a machine learning approach to the analysis of T2-weighted MRI has also been proposed as a means of evaluating macroadenoma consistency (and hence potential ease of resection) before surgery.²² If substantiated in larger studies, wider rollout of automated image analysis techniques could enable a more personalized approach to initial management and follow-up, using protocols for image acquisition that are already well established in most centers.

MOLECULAR (FUNCTIONAL) IMAGING

Molecular (functional) imaging is an important diagnostic pathway for several endocrine disorders: for example, technetium 99m (^{99m}Tc)-pertechnetate scintigraphy in

hyperthyroidism; ^{99m}Tc -sestamibi scintigraphy/single-photon emission computed tomography (SPECT) in hyperparathyroidism; indium-111 (^{111}In)-pentetate or (^{99m}Tc)-HYNIC-Ty3-octreotide scintigraphy/SPECT, or Gallium-68 (^{68}Ga)-DOTATATE positron emission tomography (PET)/CT in neuroendocrine tumours (NETs). In addition to identifying the cause/localizing sites of abnormal functioning tissue, in some instances, it can also inform treatment decisions (for example, use of lutetium-177-DOTATATE therapy in patients with metastatic NETs).

In contrast, molecular imaging has not traditionally been considered part of the diagnostic armamentarium for de novo or recurrent PA. Although several groups have explored tracers targeting different cellular pathways and receptor expression, the limitations associated with imaging the sella and parasellar regions using scintigraphy or CT have proved a significant challenge for both accurate PA localization and discrimination of tumor from remaining normal pituitary tissue. However, several recent advances, including coregistration of high-resolution PET-CT with volumetric (1-mm slice) MRI (PET/MR^{CR}) and the advent of PET/MR scanners, have allowed for more accurate localization of the site or sites of tracer uptake and differentiation from physiologic uptake by the remaining normal pituitary gland.

Somatostatin Receptor Imaging

Earlier attempts at imaging PA using tracers targeting somatostatin receptors faltered on several counts, including the relatively poor spatial resolution of scintigraphy (even when combined with CT), variable somatostatin receptor expression of individual tumors, and competing background uptake by normal pituitary tissue. More recently, studies using ^{68}Ga -DOTATATE and ^{68}Ga -DOTATOC have shown greater promise, benefiting from the significantly improved spatial resolution offered by PET. Intriguingly, in 1 study, lower tracer uptake was observed in clinically nonfunctioning PA (7 SF-1 and 2 T-Pit staining tumors) when compared with normal pituitary gland.²³ Moreover, comparing and contrasting appearances from ^{68}Ga -DOTATATE PET with those of ^{18}F -fluorodeoxyglucose (^{18}F -FDG)-PET has been proposed as a means of differentiating recurrent/residual PA from normal pituitary tissue^{24,25} and may also inform decision making for aggressive pituitary tumors.^{26,27}

Dopamine Receptor Imaging

Prolactin secretion from normal lactotrophs is subject to tonic dopaminergic inhibition, which is predominantly mediated by the dopamine receptor subtype 2.²⁸ Although several high-affinity ligands for the D2 receptor, which have been used for PET imaging in other clinical contexts (eg, psychiatric disorders), have been deployed for imaging PA,^{29,30} to date they have failed to find a role in routine pituitary practice. In part, this likely reflects the relatively limited utility of functional imaging in tumors that are predominantly managed medically, with a high expectation of dopamine agonist (DA) sensitivity. In contrast, in acromegaly, where only approximately 1 in 4 somatotroph adenomas respond to DA therapy, a functional imaging modality capable of predicting response to treatment (as reflected by focal PET tracer uptake) could represent a useful addition to the diagnostic algorithm when considering which patients might benefit from a trial of DA for persistent residual disease.

Fluorine-18-Fluorodeoxyglucose PET

^{18}F -FDG is a well-established PET tracer that finds widespread use in clinical oncology. Importantly, in a large retrospective study, which assessed pituitary uptake in 40,967 subjects undergoing ^{18}F -FDG PET/CT for other indications, focal increased tracer uptake in the pituitary fossa was observed in just 0.073% of cases, several of

Table 2		
Alternative magnetic resonance sequences/techniques for pituitary imaging		
Indications	MR Sequence/Technique	References
A: Aid to diagnosis		
Distinguish normal pituitary gland from PA or cyst	Magnetic resonance spectroscopy (MRS) Golden-angle radial sparse parallel MRI (GRASP)	63–65
Distinguish PA from vascular lesions (eg, aneurysm, meningioma)	Magnetic resonance angiography (MRA) Perfusion-weighted imaging (PWI)	66 67,68
Detection of apoplexy and cystic lesions	Diffusion-weighted imaging (DWI)	69,70
Localization of corticotroph tumors	7 T (ultra-high field) MRI Fluid-attenuation inversion recovery (FLAIR) Constructive interference in steady state (CISS ^a)	71–74
B: Preoperative assessment		
Assessment of tumor consistency	Contrast-enhanced fast imaging employing steady-state acquisition (FIESTA) Magnetic resonance elastography (MRE) Apparent diffusion coefficient (ADC, a subtype of DWI)	75 76 77–83
Assessment of tumor vascularity	PWI	84
Delineation of cavernous sinus structures/tumor invasion	MRA	85,86
Delineation of visual pathways (including optic nerve tractography)	Contrast-enhanced FIESTA 3-Dimensional CISS ^a Diffusion tensor imaging (DTI, an extension of DWI)	87 88 89–91
C: Prediction of treatment outcome		
Response to SSA therapy	MRS	92
Visual outcomes following pituitary surgery	DTI	91
Successful tumor resection at TSS	Apparent diffusion coefficient (ADC, a subtype of DWI)	80,93

^a CISS denotes a T2 gradient echo sequence.
Data from Refs. 63–93

whom were subsequently shown to have PA³¹; in a second study with a smaller sample size (13,145 subjects), incidental pituitary uptake was noted in 0.8% of subjects, although a significant proportion of these were not confirmed to represent pathologic uptake on subsequent assessment.³² Together, these studies point to a likely low risk of false positive scans (<1%) and highlight the importance of referral for endocrine assessment in any patient with incidentally detected pituitary ¹⁸F-FDG uptake. In

keeping with this, the literature contains numerous examples of different PA subtypes discovered incidentally during ^{18}F -FDG PET/CT (nonfunctioning PA,^{33–35} prolactinoma,³⁶ gonadotropinoma,³⁷ somatotropinoma,^{38,39} and corticotropinoma⁴⁰).

A role for ^{18}F -FDG PET in the detection of de novo and residual/recurrent PA has been explored by several groups. In a prospective study of 24 patients with different subtypes of PA, all macroadenomas ($n = 14$) and half of microadenomas ($n = 5$) demonstrated increased tracer uptake.⁴¹ As outlined previously, ^{18}F -FDG PET may also help distinguish residual or recurrent adenoma from remaining normal pituitary tissue following TSS when combined with ^{68}Ga -DOTATATE PET.²⁴

However, perhaps the greatest interest in the application of ^{18}F -FDG PET in the management of pituitary disease has been in Cushing disease, whereby 30% to 40% of microadenomas may go unidentified on standard clinical MRI. In a study of 12 patients with pituitary Cushing, ^{18}F -FDG PET was found to be comparable to MRI for the localization of corticotroph adenomas with a detection rate of approximately 60%, albeit without complete overlap between the 2 imaging modalities.⁴² In a prospective study of 10 patients with Cushing disease, Chittiboina and colleagues⁴³ were able to show slight superiority of ^{18}F -FDG PET in comparison with conventional SE MRI but, in the same cohort, SPGR MRI was superior to ^{18}F -FDG PET. However, more recently the same group has shown that prior stimulation with corticotropin-releasing hormone may enhance the ability of ^{18}F -FDG PET to detect corticotropinomas.⁴⁴

Nitrogen-13-Ammonia PET

^{13}N -ammonia has previously been proposed as a marker of pituitary gland perfusion and metabolism, which allows the localization of normal functioning tissue, with reduced/absent uptake following pituitary injury.⁴⁵ Perhaps mirroring this, in a single study of ^{13}N -ammonia PET/CT in 48 patients with different PA subtypes (22 non-functioning PA (NFPA), 12 acromegaly, 10 Cushing disease, 4 prolactinomas), higher tracer uptake was observed in normal residual pituitary tissue compared with adenoma (which contrasted with findings on ^{18}F -FDG PET/CT).⁴⁶ However, the ability of ^{13}N -ammonia PET/CT to identify the site of normal pituitary tissue was diminished when the maximal tumor diameter exceeded 2 cm.⁴⁶

Fluorine-18-Choline PET

^{18}F -Choline, a PET tracer used in the staging and restaging of prostate cancer, is taken up by the normal pituitary gland,^{47,48} raising the possibility of a role in imaging PA. However, to date, support for such a role is limited to a small number of case reports of incidentally detected pituitary macroadenomas.^{49,50} It is also unclear whether uptake in PA is dependent on cellular proliferation (with incorporation into cell membranes) or reflects other aspects of choline transport/metabolism, as has been proposed for other well-differentiated endocrine tumors.⁵¹

Carbon-11-Methionine PET

The hallmark of PA is inappropriate peptide synthesis, even in clinically nonfunctioning tumors of the gonadotrope (SF-1) lineage. Accordingly, molecular imaging using a labeled amino acid PET tracer has the immediate attraction of potentially finding application in all PA subtypes. To date, the most studied amino acid tracer in PA is ^{11}C -methionine, which benefits from considerably lower brain uptake (producing a more favorable target-to-background ratio), and increased sensitivity for the detection of PA, when compared with ^{18}F -FDG.^{52–54}

Perhaps the single most important recent advance in pituitary imaging using ^{11}C -methionine has been the move to routine coregistration of PET/CT and MRI images

(Met-PET/MRI^{CR}), which allows (i) more accurate (anatomic) localization of the site or sites of methionine uptake, and (ii) more reliable distinction between tumoral and normal pituitary tissue tracer uptake^{12,54–56}; the advent of PET/MR hybrid scanners will likely further capitalize on these advances.

As with other functional imaging modalities, biochemical assessment of disease status should be performed on the day of the ¹¹C-methionine scan. In addition, patients treated with agents that suppress tumor function require a period of medication washout before imaging (eg, 3 months for somatostatin analogue therapy [SSA] therapy; 4 weeks for DA therapy).

Currently, there are 2 main clinical scenarios when Met-PET/MRI^{CR} should be considered:

- A. In de novo pituitary disease when targeted intervention (eg, TSS or stereotactic radiosurgery) is being considered, but MRI is either “negative” or equivocal.
- B. In patients with persistent/recurrent disease following previous intervention (surgery ± radiotherapy/radiosurgery ± medical therapy), when further targeted intervention would be considered but MRI is unable to reliably identify the site or sites of residual/recurrent disease and/or distinguish from posttreatment change.

Patients in group A include up to 30% of patients with Cushing disease (Fig. 2), occasional patients with acromegaly owing to an occult microadenoma (Fig. 3), some thyrotropinomas, and a small group of prolactinomas with DA resistance and/or intolerance.^{56,57}

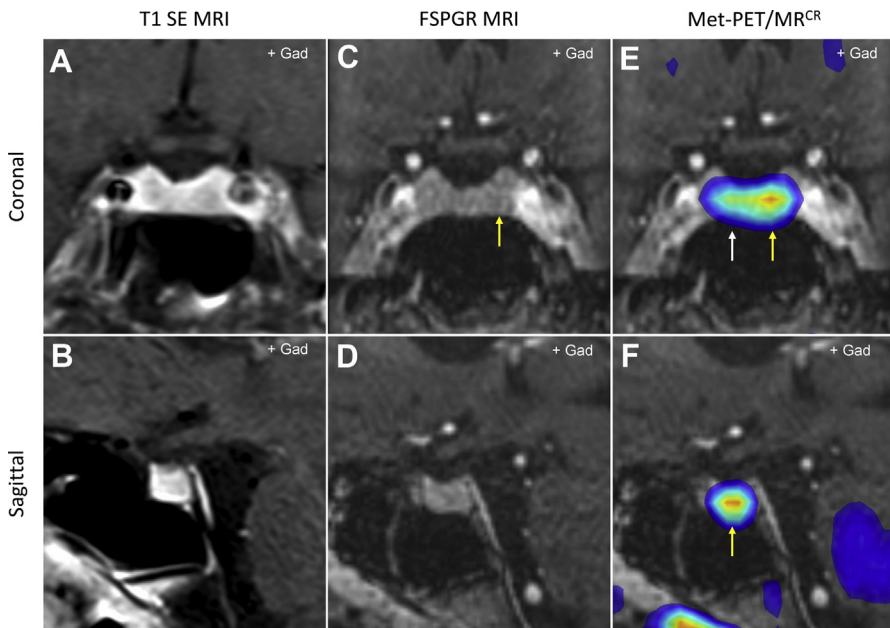


Fig. 2. Identification of the site of an occult microadenoma in Cushing disease. (A, B) T1 SE MRI is unable to identify a discrete adenoma. (C, D) Volumetric (FSPGR) MRI is also equivocal, but raises the possibility of a subtle area of hypoattenuation in the left side of the gland (yellow arrow). (E, F) Met-PET/MR^{CR} demonstrates focal increased tracer uptake (yellow arrow) corresponding to the area seen on volumetric MRI (and subsequently confirmed at TSS); normal physiologic tracer uptake is seen in the right side of the gland (white arrow).

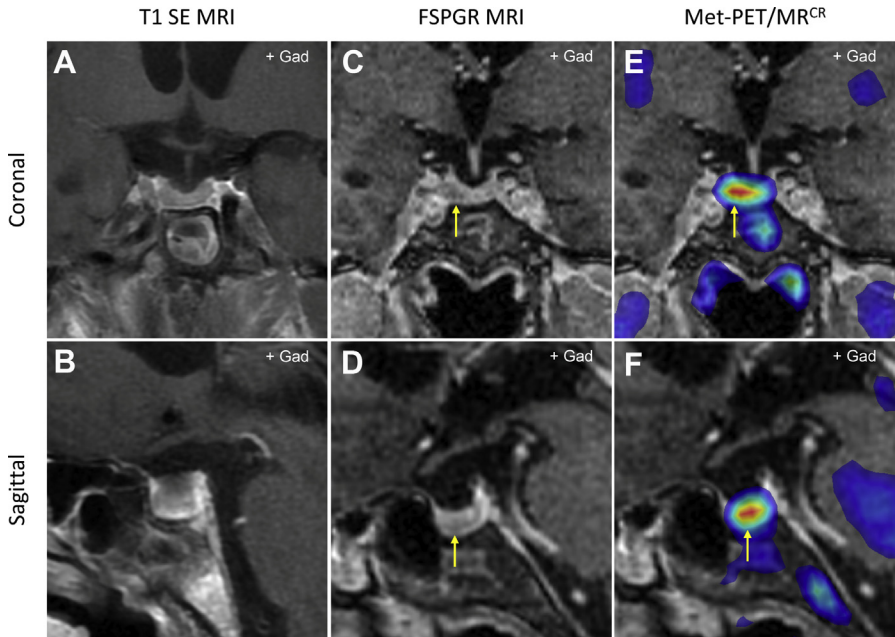


Fig. 3. Identification of the site of an occult microadenoma in acromegaly. (A, B) T1 SE MRI demonstrates equivocal findings with no discrete adenoma visualized. (C, D) Volumetric (FSPGR) MRI identifies a 5-mm focal hypointensity in the right inferior aspect of the gland (*arrow*) suggestive of a microadenoma. (E, F) Met-PET/MR^{CR} reveals an area of focal high tracer uptake (*arrow*) at the site of the suspected microadenoma.

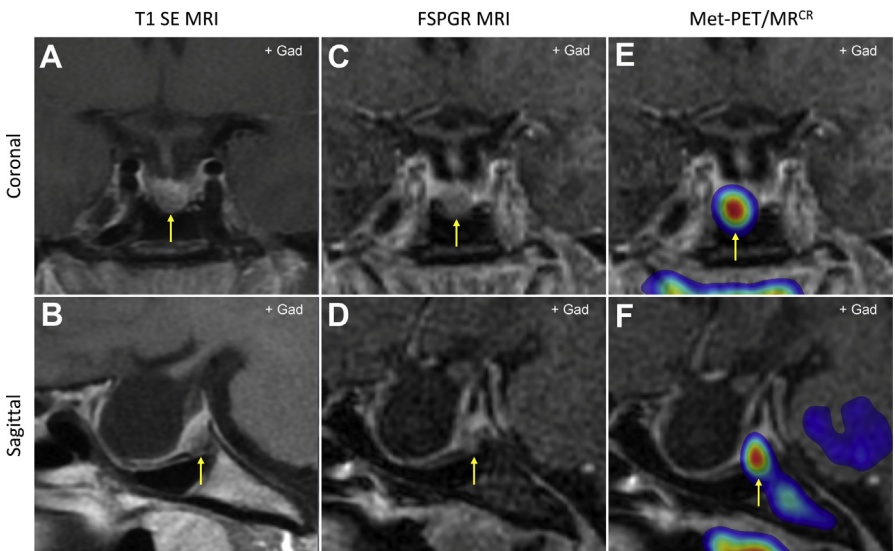


Fig. 4. Localization of the site of early recurrence (at 8 months) following primary surgery in a patient with acromegaly (sparsely granulated tumor; MIB-1 proliferation index = 15%). (A, B) T1 SE MRI shows a largely empty sella, but with a possible area of abnormal tissue posterior to the site of insertion of the infundibulum (*arrow*). (C, D) Volumetric (FSPGR) MRI demonstrates a similar appearance. (E, F) Met-PET/MR^{CR} shows focal high tracer uptake at the suspected site of recurrence (confirmed at repeat TSS).

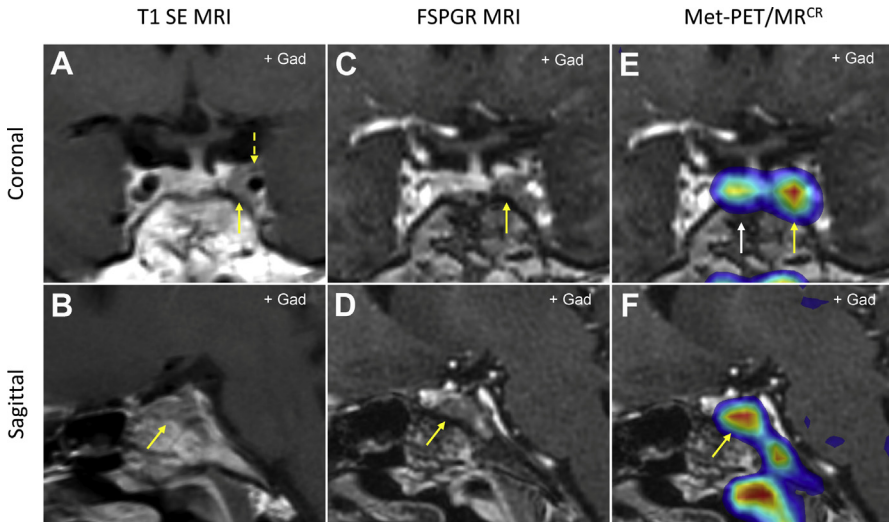


Fig. 5. Localization of the site of late recurrence (at 48 months) following primary surgery in a patient with Cushing disease. (A, B) T1 SE MRI demonstrates an area of hypointensity adjacent to (yellow arrow), and possibly invading (yellow dashed arrow), the left cavernous sinus. (C, D) Volumetric (FSPGR) MRI suggests the area of abnormal signal lies medial to the cavernous sinus. (E, F) Met-PET/MR^{CR} shows focal high tracer uptake that corresponds with the findings of FSPGR MRI (confirmed at repeat TSS with complete postoperative biochemical remission); normal physiologic tracer uptake is seen in the right side of the gland (white arrow).

Although all PA subtypes may be represented in group B, persistence or recurrence of hypercortisolism or acromegaly is the most common reason for referral to the authors' center for Met-PET/MRI^{CR} (Figs. 4 and 5).^{12,56} Importantly, a significant proportion of patients with acromegaly who were previously deemed unsuitable for further surgical intervention can be offered a repeat transsphenoidal approach following Met-PET/MRI^{CR} with the expectation of achieving full remission or a significant improvement in disease control.¹² More recently, the authors have also shown that subjects with suspected lateral sellar/parasellar disease may derive particular benefits from such an approach.⁵⁸

SUMMARY

For most patients diagnosed with a PA, good-quality T1- (\pm contrast enhancement) and T2-weighted MRI sequences will provide all of the information that is required to facilitate effective and timely decision making. However, imaging of pituitary tumors is an evolving field, both in response to and as a driver of, developments in surgical, radiotherapeutic, and pharmacologic management strategies. Increasing use of alternative MR sequences may aid localization of small functional tumors. Advances in analysis of MRI characteristics have the potential to predict tumor type and response to medical treatment. Molecular (functional) imaging, most clearly demonstrated to date with ¹¹C-methionine PET (Met-PET/MR^{CR}), is potentially able to facilitate curative surgery/radiotherapy (with minimum disruption of normal pituitary function) in an increasing number of scenarios, in both de novo and residual/recurrent pituitary disease. Molecular imaging may also be an aid in predicting response to specific medical

therapies. In an era of personalized, precision medicine, imaging has an important and increasing role in decision making in pituitary disease.

DISCLOSURE

The authors have nothing to disclose.

REFERENCES

1. Melmed S. Pituitary-tumor endocrinopathies. *N Engl J Med* 2020;382(10):937–50. Longo DL, ed.
2. Molitch ME. Pituitary incidentalomas. *Best Pract Res Clin Endocrinol Metab* 2009; 23(5):667–75.
3. Hall WA. Pituitary magnetic resonance imaging in normal human volunteers: occult adenomas in the general population. *Ann Intern Med* 1994;120(10):817.
4. Chong BW, Kucharczyk W, Singer W, et al. Pituitary gland MR: a comparative study of healthy volunteers and patients with microadenomas. *Am J Neuroradiol* 1994;15(4):675–9. Available at: <http://www.ncbi.nlm.nih.gov/pubmed/8010269>.
5. Vasilev V, Rostomyan L, Daly AF, et al. Pituitary “incidentaloma”: neuroradiological assessment and differential diagnosis. *Eur J Endocrinol* 2016;175(4):R171–84.
6. Daly AF, Rixhon M, Adam C, et al. High prevalence of pituitary adenomas: a cross-sectional study in the province of Liège, Belgium. *J Clin Endocrinol Metab* 2006;91(12):4769–75.
7. Fernandez A, Karavitaki N, Wass JAH. Prevalence of pituitary adenomas: a community-based, cross-sectional study in Banbury (Oxfordshire, UK). *Clin Endocrinol (Oxf)* 2010. <https://doi.org/10.1111/j.1365-2265.2009.03667.x>.
8. Casanueva FF, Barkan AL, Buchfelder M, et al. Criteria for the definition of pituitary tumor centers of excellence (PTCOE): a pituitary society statement. *Pituitary* 2017;20(5):489–98.
9. Pressman BD. Pituitary imaging. *Endocrinol Metab Clin North Am* 2017;46(3): 713–40.
10. Bashari WA, Senanayake R, Fernández-Pombo A, et al. Modern imaging of pituitary adenomas. *Best Pract Res Clin Endocrinol Metab* 2019;33(2):101278.
11. Erickson D, Erickson B, Watson R, et al. 3 Tesla magnetic resonance imaging with and without corticotropin releasing hormone stimulation for the detection of microadenomas in Cushing’s syndrome. *Clin Endocrinol (Oxf)* 2010;72(6):793–9.
12. Koulouri O, Kandasamy N, Hoole AC, et al. Successful treatment of residual pituitary adenoma in persistent acromegaly following localisation by 11C-methionine PET co-registered with MRI. *Eur J Endocrinol* 2016;175(5):485–98.
13. Bonneville J-F. Magnetic resonance imaging of pituitary tumors. *Front Horm Res* 2016;45:97–120.
14. Bonneville JF, Bonneville F, Cattin F. Magnetic resonance imaging of pituitary adenomas. *Eur Radiol* 2005;15(3):543–8.
15. Kasaliwal R, Sankhe SS, Lila AR, et al. Volume interpolated 3D-spoiled gradient echo sequence is better than dynamic contrast spin echo sequence for MRI detection of corticotropin secreting pituitary microadenomas. *Clin Endocrinol (Oxf)* 2013;78(6):825–30.
16. Grober Y, Grober H, Wintermark M, et al. Comparison of MRI techniques for detecting microadenomas in Cushing’s disease. *J Neurosurg* 2018;128(4):1051–7.
17. McDonald RJ, McDonald JS, Kallmes DF, et al. Gadolinium deposition in human brain tissues after contrast-enhanced MR imaging in adult patients without intracranial abnormalities. *Radiology* 2017;285(2):546–54.

18. Bussi S, Coppo A, Botteron C, et al. Differences in gadolinium retention after repeated injections of macrocyclic MR contrast agents to rats. *J Magn Reson Imaging* 2018;47(3):746–52.
19. Nachtigall LB, Karavitaki N, Kiseljak-Vassiliades K, et al. Physicians' awareness of gadolinium retention and MRI timing practices in the longitudinal management of pituitary tumors: a "Pituitary Society" survey. *Pituitary* 2019;22(1):37–45.
20. Bonneville J-F. A plea for the T2W MR sequence for pituitary imaging. *Pituitary* 2019;22(2):195–7.
21. Ugga L, Cuocolo R, Solari D, et al. Prediction of high proliferative index in pituitary macroadenomas using MRI-based radiomics and machine learning. *Neuroradiology* 2019;61(12):1365–73.
22. Zeynalova A, Kocak B, Durmaz ES, et al. Preoperative evaluation of tumour consistency in pituitary macroadenomas: a machine learning-based histogram analysis on conventional T2-weighted MRI. *Neuroradiology* 2019;61(7):767–74.
23. Tjörnstrand A, Casar-Borota O, Heurling K, et al. Lower 68 Ga-DOTATOC uptake in nonfunctioning pituitary neuroendocrine tumours compared to normal pituitary gland—a proof-of-concept study. *Clin Endocrinol (Oxf)* 2019. <https://doi.org/10.1111/cen.14144>.
24. Zhao X, Xiao J, Xing B, et al. Comparison of (68)Ga DOTATATE to 18F-FDG uptake is useful in the differentiation of residual or recurrent pituitary adenoma from the remaining pituitary tissue after transsphenoidal adenomectomy. *Clin Nucl Med* 2014;39(7):605–8.
25. Wang H, Hou B, Lu L, et al. PET/MRI in the diagnosis of hormone-producing pituitary microadenoma: a prospective pilot study. *J Nucl Med* 2018;59(3):523–8.
26. Xiao J, Zhu Z, Zhong D, et al. Improvement in diagnosis of metastatic pituitary carcinoma by 68Ga DOTATATE PET/CT. *Clin Nucl Med* 2015;40(2):e129–31.
27. Garmes HM, Carvalheira JBC, Reis F, et al. Pituitary carcinoma: a case report and discussion of potential value of combined use of Ga-68 DOTATATE and F-18 FDG PET/CT scan to better choose therapy. *Surg Neurol Int* 2017;8:162.
28. Ferone D, Pivonello R, Lastoria S, et al. In vivo and in vitro effects of octreotide, quinagolide and cabergoline in four hyperprolactinaemic acromegalics: correlation with somatostatin and dopamine D2 receptor scintigraphy. *Clin Endocrinol (Oxf)* 2001;54(4):469–77. Available at: <http://www.ncbi.nlm.nih.gov/pubmed/11318782>.
29. Muhr C. Positron emission tomography in acromegaly and other pituitary adenoma patients. *Neuroendocrinology* 2006;83(3–4):205–10.
30. Bergström M, Muhr C, Lundberg PO, et al. PET as a tool in the clinical evaluation of pituitary adenomas. *J Nucl Med* 1991;32(4):610–5. Available at: <http://www.ncbi.nlm.nih.gov/pubmed/2013801>.
31. Jeong SY, Lee S-W, Lee HJ, et al. Incidental pituitary uptake on whole-body 18F-FDG PET/CT: a multicentre study. *Eur J Nucl Med Mol Imaging* 2010;37(12):2334–43.
32. Hyun SH, Choi JY, Lee K-H, et al. Incidental focal 18F-FDG uptake in the pituitary gland: clinical significance and differential diagnostic criteria. *J Nucl Med* 2011;52(4):547–50.
33. Maffei P, Marzola MC, Musto A, et al. A very rare case of nonfunctioning pituitary adenoma incidentally disclosed at 18F-FDG PET/CT. *Clin Nucl Med* 2012;37(5):e100–1.
34. Campeau RJ, David O, Dowling AM. Pituitary adenoma detected on FDG positron emission tomography in a patient with mucosa-associated lymphoid tissue lymphoma. *Clin Nucl Med* 2003;28(4):296–8.

35. Karapolat İ, Öncel G, Kumanlioğlu K. Clinically occult pituitary adenoma can appear as a hypermetabolic lesion on whole body FDG PET imaging in a patient with lymphoma. *Molecular Imaging Radionucl Ther* 2013;22(1):18–20.
36. Gemmel F, Balink H, Collins J, et al. Occult prolactinoma diagnosed by FDG PET/CT. *Clin Nucl Med* 2010;35(4):269–70.
37. Joshi P, Lele V, Gandhi R. Incidental detection of clinically occult follicle stimulating hormone secreting pituitary adenoma on whole body 18-fluorodeoxyglucose positron emission tomography-computed tomography. *Indian J Nucl Med* 2011;26(1):34–5.
38. Koo CW, Bhargava P, Rajagopalan V, et al. Incidental detection of clinically occult pituitary adenoma on whole-body FDG PET imaging. *Clin Nucl Med* 2006;31(1):42–3.
39. Maiza J-C, Zunic P, Revel C, et al. Acromegaly revealed by 18FDG-PET/CT in a plasmocytoma patient. *Pituitary* 2012;15(4):614–5.
40. Komori T, Martin WH, Graber AL, et al. Serendipitous detection of Cushing's disease by FDG positron emission tomography and a review of the literature. *Clin Nucl Med* 2002;27(3):176–8.
41. Seok H, Lee EJY, Choe EY, et al. Analysis of 18F-fluorodeoxyglucose positron emission tomography findings in patients with pituitary lesions. *Korean J Intern Med* 2013;28(1):81–8.
42. Alzahrani AS, Farhat R, Al-Arifi A, et al. The diagnostic value of fused positron emission tomography/computed tomography in the localization of adrenocorticotropin-secreting pituitary adenoma in Cushing's disease. *Pituitary* 2009;12(4):309–14.
43. Chittiboina P, Montgomery BK, Millo C, et al. High-resolution 18F-fluorodeoxyglucose positron emission tomography and magnetic resonance imaging for pituitary adenoma detection in Cushing disease. *J Neurosurg* 2015;122(4):791–7.
44. Boyle J, Patronas NJ, Smirniotopoulos J, et al. CRH stimulation improves 18F-FDG-PET detection of pituitary adenomas in Cushing's disease. *Endocrine* 2019;65(1):155–65.
45. Xiangsong Z, Dianchao Y, Anwu T. Dynamic 13N-ammonia PET: a new imaging method to diagnose hypopituitarism. *J Nucl Med* 2005;46(1):44–7.
46. Wang Z, Mao Z, Zhang X, et al. Utility of 13N-ammonia PET/CT to detect pituitary tissue in patients with pituitary adenomas. *Acad Radiol* 2019;26(9):1222–8.
47. Haroon A, Zaroni L, Celli M, et al. Multicenter study evaluating extraprostatic uptake of 11C-choline, 18F-methylcholine, and 18F-ethylcholine in male patients: physiological distribution, statistical differences, imaging pearls, and normal variants. *Nucl Med Commun* 2015;36(11):1065–75. Available at: https://journals.lww.com/nuclearmedicinecomm/Fulltext/2015/11000/Multicenter_study_evaluating_extraprostatic_uptake.1.aspx.
48. Schillaci O, Calabria F, Tavolozza M, et al. 18F-choline PET/CT physiological distribution and pitfalls in image interpretation: experience in 80 patients with prostate cancer. *Nucl Med Commun* 2010;31(1):39–45.
49. Maffione AM, Mandoliti G, Pasini F, et al. Pituitary non-functioning adenoma disclosed at 18F-choline PET/CT to investigate a prostate cancer relapse. *Clin Nucl Med* 2016;41(10):e460–1.
50. Albano D, Bosio G, Bertagna F. Incidental pituitary adenoma detected by 18 F-FDG PET/CT and 18 F-choline PET/CT in the same patient. *Rev Esp Med Nucl Imagen Mol* 2018;37(4):250–2.

51. van der Hiel B, Stokkel MPM, Buikhuisen WA, et al. 18F-Choline PET/CT as a new tool for functional imaging of non-proliferating secreting neuroendocrine tumors. *J Endocrinol Metab* 2015;5(4):267–71.
52. Feng Z, He D, Mao Z, et al. Utility of 11C-methionine and 18F-FDG PET/CT in patients with functioning pituitary adenomas. *Clin Nucl Med* 2016;41(3):e130–4.
53. Tomura N, Saginoya T, Mizuno Y, et al. Accumulation of 11 C-methionine in the normal pituitary gland on 11 C-methionine PET. *Acta Radiol* 2017;58(3):362–6.
54. Ikeda H, Abe T, Watanabe K. Usefulness of composite methionine–positron emission tomography/3.0-Tesla magnetic resonance imaging to detect the localization and extent of early-stage Cushing adenoma. *J Neurosurg* 2010;112(4):750–5.
55. Rodriguez-Barcelo S, Gutierrez-Cardo A, Dominguez-Paez M, et al. Clinical usefulness of coregistered 11C-methionine positron emission tomography/3-T magnetic resonance imaging at the follow-up of acromegaly. *World Neurosurg* 2014; 82(3–4):468–73.
56. Koulouri O, Steuwe A, Gillett D, et al. A role for 11C-methionine PET imaging in ACTH-dependent Cushing’s syndrome. *Eur J Endocrinol* 2015;173(4):M107–20.
57. Koulouri O, Hoole AC, English P, et al. Localisation of an occult thyrotropinoma with 11 C-methionine PET-CT before and after somatostatin analogue therapy. *Lancet Diabetes Endocrinol* 2016;4(12):1050.
58. Bashari W, Senanayake R, Koulouri O, et al. PET-guided repeat transsphenoidal surgery for previously deemed unresectable lateral disease in acromegaly. *Neurosurg Focus* 2020;48(6):E8.
59. Potorac I, Beckers A, Bonneville J-F. T2-weighted MRI signal intensity as a predictor of hormonal and tumoral responses to somatostatin receptor ligands in acromegaly: a perspective. *Pituitary* 2017;20(1):116–20.
60. Heck A, Emblem KE, Casar-Borota O, et al. Quantitative analyses of T2-weighted MRI as a potential marker for response to somatostatin analogs in newly diagnosed acromegaly. *Endocrine* 2016;52(2):333–43.
61. Varlamov EV, Hinojosa-Amaya JM, Fleseriu M. Magnetic resonance imaging in the management of prolactinomas; a review of the evidence. *Pituitary* 2020; 23(1):16–26.
62. Cazabat L, Dupuy M, Boulin A, et al. Silent, but not unseen: multimicrocystic aspect on T2-weighted MRI in silent corticotroph adenomas. *Clin Endocrinol (Oxf)* 2014;81(4):566–72.
63. Chernov MF, Kawamata T, Amano K, et al. Possible role of single-voxel 1H-MRS in differential diagnosis of suprasellar tumors. *J Neurooncol* 2009;91(2):191–8.
64. Pînzariu O, Georgescu B, Georgescu CE. Metabolomics—a promising approach to pituitary adenomas. *Front Endocrinol (Lausanne)* 2019;9:814.
65. Hainc N, Stippich C, Reinhardt J, et al. Golden-angle radial sparse parallel (GRASP) MRI in clinical routine detection of pituitary microadenomas: first experience and feasibility. *Magn Reson Imaging* 2019;60:38–43.
66. Manara R, Maffei P, Citton V, et al. Increased rate of intracranial saccular aneurysms in acromegaly: an MR angiography study and review of the literature. *J Clin Endocrinol Metab* 2011;96(5):1292–300.
67. Hakyemez B, Yildirim N, Erdodañ C, et al. Meningiomas with conventional MRI findings resembling intraaxial tumors: can perfusion-weighted MRI be helpful in differentiation? *Neuroradiology* 2006;48(10):695–702.
68. Bladowska J, Zimny A, Guziński M, et al. Usefulness of perfusion weighted magnetic resonance imaging with signal-intensity curves analysis in the differential diagnosis of sellar and parasellar tumors: preliminary report. *Eur J Radiol* 2013; 82(8):1292–8.

69. Rogg JM, Tung GA, Anderson G, et al. Pituitary apoplexy: early detection with diffusion-weighted MR imaging. *AJNR Am J Neuroradiol* 2002;23(7):1240–5. Available at: <http://www.ncbi.nlm.nih.gov/pubmed/12169486>. Accessed April 23, 2019.
70. Kunii N, Abe T, Kawamo M, et al. Rathke's cleft cysts: differentiation from other cystic lesions in the pituitary fossa by use of single-shot fast spin-echo diffusion-weighted MR imaging. *Acta Neurochir (Wien)* 2007;149(8):759–69.
71. de Rotte AAJ, Groenewegen A, Rutgers DR, et al. High resolution pituitary gland MRI at 7.0 Tesla: a clinical evaluation in Cushing's disease. *Eur Radiol* 2016;26(1):271–7.
72. Patel V, Liu CSJ, Shiroishi MS, et al. Ultra-high field magnetic resonance imaging for localization of corticotropin-secreting pituitary adenomas. *Neuroradiology* 2020.
73. Chatain GP, Patronas N, Smirniotopoulos JG, et al. Potential utility of FLAIR in MRI-negative Cushing's disease. *J Neurosurg* 2018;129(3):620–8.
74. Lang M, Habboub G, Moon D, et al. Comparison of constructive interference in steady-state and T1-weighted MRI sequence at detecting pituitary adenomas in Cushing's disease patients. *J Neurol Surg B Skull Base* 2018;79(06):593–8.
75. Yamamoto J, Kakeda S, Shimajiri S, et al. Tumor consistency of pituitary macroadenomas: predictive analysis on the basis of imaging features with contrast-enhanced 3D FIESTA at 3T. *Am J Neuroradiol* 2014;35(2):297–303.
76. Hughes JD, Fattahi N, Van Gompel J, et al. Magnetic resonance elastography detects tumoral consistency in pituitary macroadenomas. *Pituitary* 2016;19(3):286–92.
77. Pierallini A, Caramia F, Falcone C, et al. Pituitary macroadenomas: preoperative evaluation of consistency with diffusion-weighted MR imaging—initial experience. *Radiology* 2006;239(1):223–31.
78. Suzuki C, Maeda M, Hori K, et al. Apparent diffusion coefficient of pituitary macroadenoma evaluated with line-scan diffusion-weighted imaging. *J Neuroradiol* 2007;34(4):228–35.
79. Mahmoud OM, Tominaga A, Amatya VJ, et al. Role of PROPELLER diffusion-weighted imaging and apparent diffusion coefficient in the evaluation of pituitary adenomas. *Eur J Radiol* 2011;80(2):412–7.
80. Alimohamadi M, Sanjari R, Mortazavi A, et al. Predictive value of diffusion-weighted MRI for tumor consistency and resection rate of nonfunctional pituitary macroadenomas. *Acta Neurochir (Wien)* 2014;156(12):2245–52.
81. Yiping L, Ji X, Daoying G, et al. Prediction of the consistency of pituitary adenoma: a comparative study on diffusion-weighted imaging and pathological results. *J Neuroradiol* 2016;43(3):186–94.
82. Wang M, Liu H, Wei X, et al. Application of reduced-FOV diffusion-weighted imaging in evaluation of normal pituitary glands and pituitary macroadenomas. *AJNR Am J Neuroradiol* 2018;39(8):1499–504.
83. Sanei Taheri M, Kimia F, Mehrnahad M, et al. Accuracy of diffusion-weighted imaging-magnetic resonance in differentiating functional from non-functional pituitary macro-adenoma and classification of tumor consistency. *Neuroradiol J* 2019;32(2):74–85.
84. Ma Z, He W, Zhao Y, et al. Predictive value of PWI for blood supply and T1-spin echo MRI for consistency of pituitary adenoma. *Neuroradiology* 2016;58(1):51–7.
85. Linn J, Peters F, Lummel N, et al. Detailed imaging of the normal anatomy and pathologic conditions of the cavernous region at 3 Tesla using a contrast-enhanced MR angiography. *Neuroradiology* 2011;53(12):947–54.

86. Micko ASG, Wöhrer A, Wolfsberger S, et al. Invasion of the cavernous sinus space in pituitary adenomas: endoscopic verification and its correlation with an MRI-based classification. *J Neurosurg* 2015;122(4):803–11.
87. Watanabe K, Kakeda S, Yamamoto J, et al. Delineation of optic nerves and chiasm in close proximity to large suprasellar tumors with contrast-enhanced FIESTA MR imaging. *Radiology* 2012;264(3):852–8.
88. Suprasanna K, Vinay Kumar KM, Kumar A, et al. Comparison of pituitary stalk angle, inter-neural angle and optic tract angle in relation to optic chiasm location on 3-dimensional magnetic resonance imaging. *J Clin Neurosci* 2019;64:169–73.
89. Yu CS, Li KC, Xuan Y, et al. Diffusion tensor tractography in patients with cerebral tumors: a helpful technique for neurosurgical planning and postoperative assessment. *Eur J Radiol* 2005;56(2):197–204.
90. Salmela MB, Cauley KA, Nickerson JP, et al. Magnetic resonance diffusion tensor imaging (MRDTI) and tractography in children with septo-optic dysplasia. *Pediatr Radiol* 2010;40(5):708–13.
91. Anik I, Anik Y, Cabuk B, et al. Visual outcome of an endoscopic endonasal trans-sphenoidal approach in pituitary macroadenomas: quantitative assessment with diffusion tensor imaging early and long-term results. *World Neurosurg* 2018;112:e691–701.
92. Hu J, Yan J, Zheng X, et al. Magnetic resonance spectroscopy may serve as a presurgical predictor of somatostatin analog therapy response in patients with growth hormone-secreting pituitary macroadenomas. *J Endocrinol Invest* 2019;42(4):443–51.
93. Hassan HA, Bessar MA, Herzallah IR, et al. Diagnostic value of early postoperative MRI and diffusion-weighted imaging following trans-sphenoidal resection of non-functioning pituitary macroadenomas. *Clin Radiol* 2018;73(6):535–41.